Supporting information

A ratiometric bioluminescent indicator for simple and rapid diagnosis of bilirubin

Yukino Itoh,[1,#] Mitsuru Hattori,[2,#] Tetsuichi Wazawa,[2] Yoshiyuki Arai,[2] and Takeharu Nagai*,[1,2]

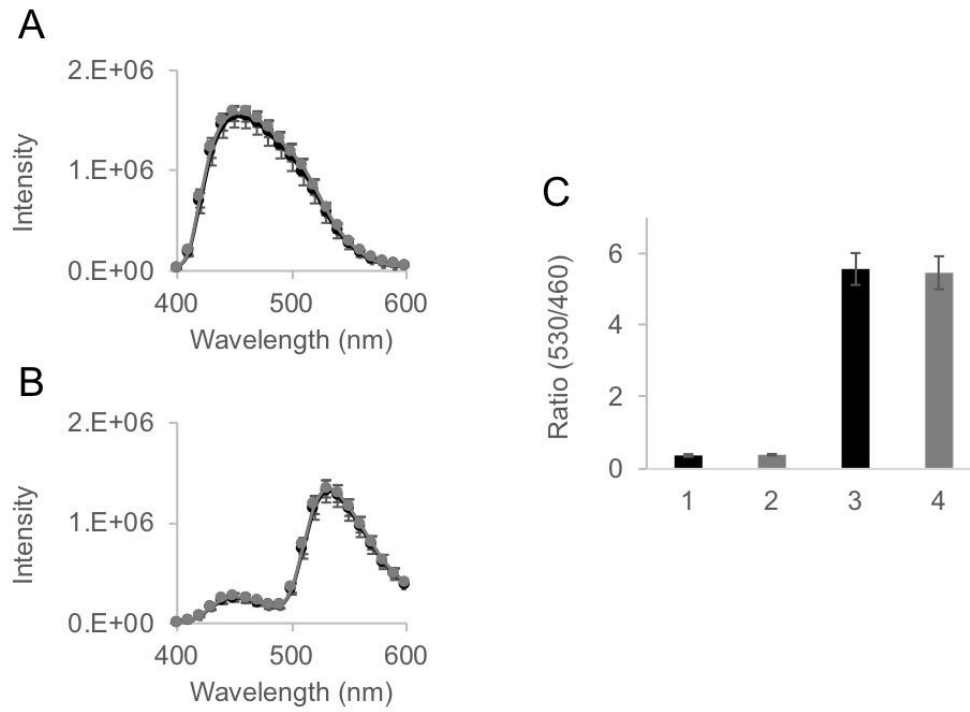[1]Graduate School of Frontier Biosciences, Osaka University, 2-1 Yamadaoka, Suita 565-0871, Japan

[2]The Institute of Scientific and Industrial Research (SANKEN), Osaka University, 8-1 Mihogaoka, Ibaraki 567-0047, Japan


*Corresponding author: Takeharu, Nagai
Phone: +81-6-6879-8480.
E-mail: ng1@sanken.osaka-u.ac.jp.

# Y.I and M.H have equally contribution to this work.

Supplemental Figure 1. Stability of BABI. The emission spectra of BABI (A) and BABI reacted with 200 μM UCBR (B). Luminescence was measured using BABI stored in -80 °C for 1 week (black) and 3 weeks (gray) after purification. Calculated ratio (530/460 nm) from A and B (C). The emission ratio of 1. BABI stored for 1 week, 2. BABI stored for 3 weeks, 3. BABI stored for 1 week with UCBR, and 4. BABI stored for 3 weeks with UCBR. The average and standard deviations are shown for $n = 3$.

A

B
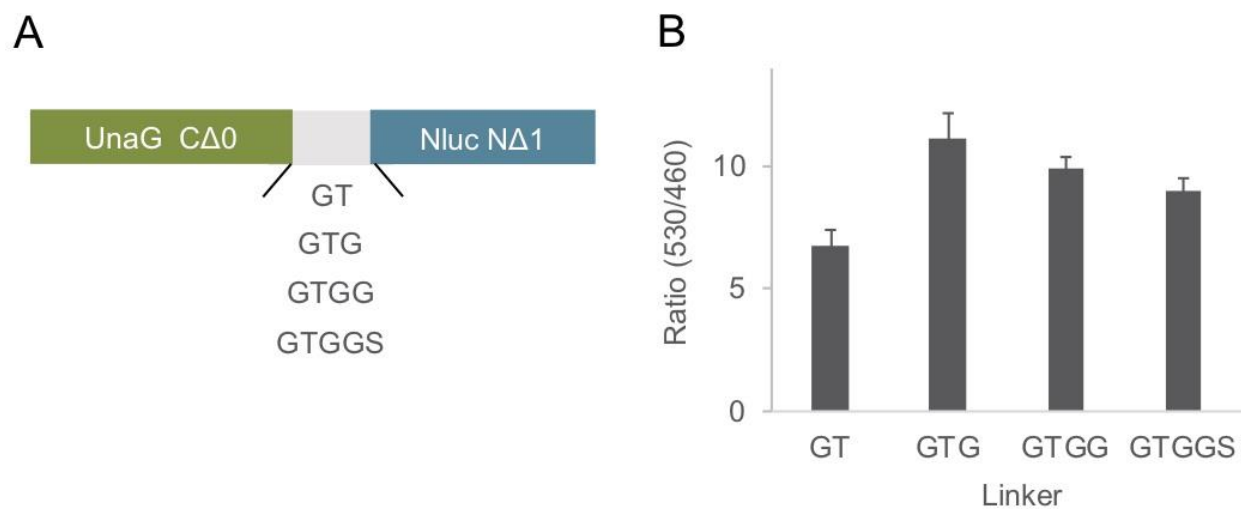
Supplemental Figure 2. Linker optimization in BABI with additional amino acids. (A) Schematic structure of BABI variants with different linker sequences. (B) Ratio of bioluminescence intensity (530/460 nm) of each variant. These counts were measured from *E. coli* colonies after reaction with UCBR. The averaged data and standard deviations are shown for *n* = 3.
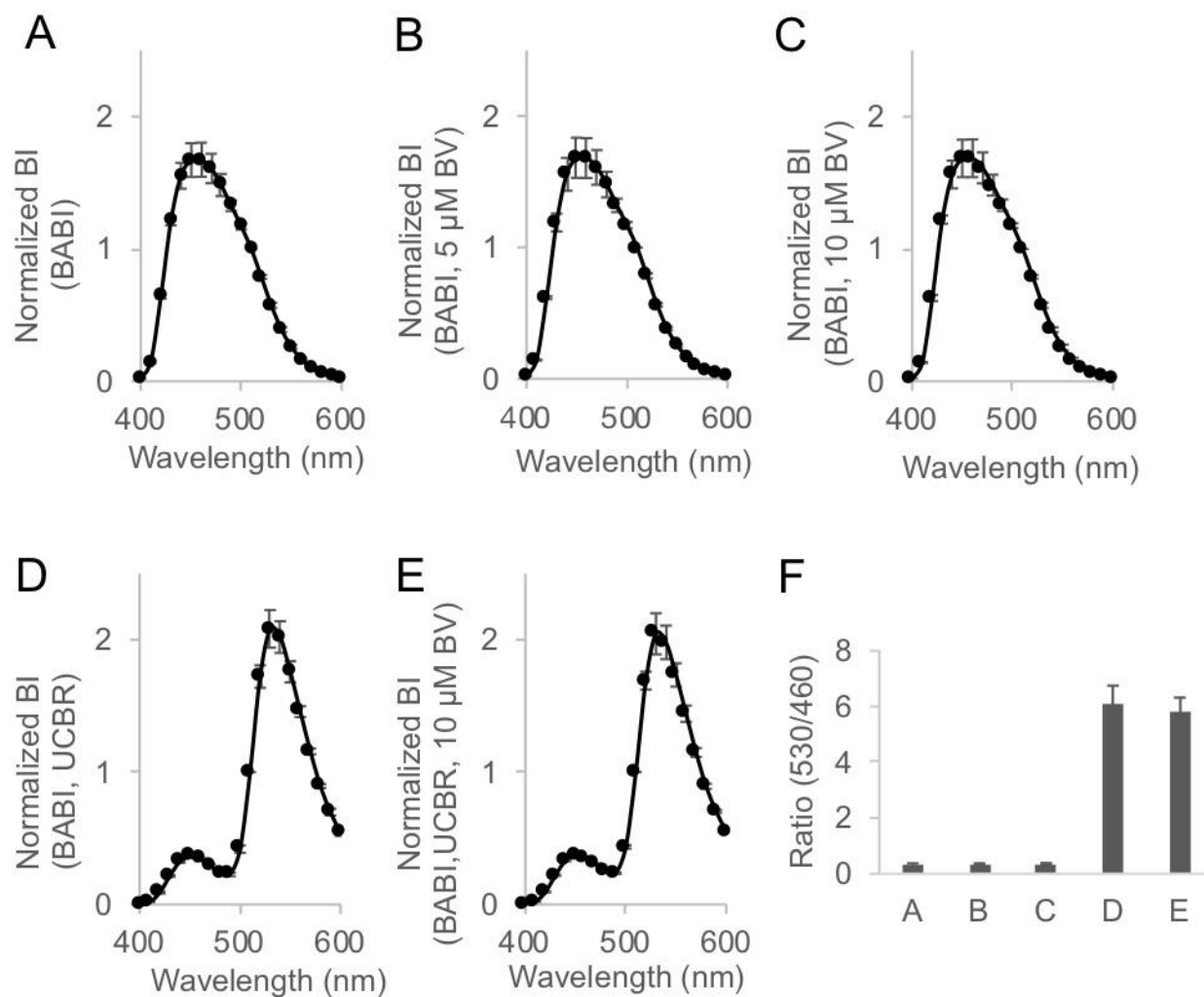
Supplemental Figure 3. Effect of biliverdin on the reaction of BABI with UCBR. (A-E) Emission spectra of BABI, BABI+5 µM biliverdin (BV), BABI+10 µM BV, BABI+200 µM UCBR, and BABI+200 µM UCBR+10 µM BV. The BV concentrations in the sample were in or higher than the range of it in newborn blood (0-6 µM).[1] The reaction condition was same with 2 µM BABI condition in Figure 3A. Bioluminescence intensities measured by a micro plate reader were normalized at the iso-emissive point (510 nm). (F) The emission ratios (530/460 nm) of BABI calculated from the spectra of A-E. The average and standard deviations are shown for n = 3
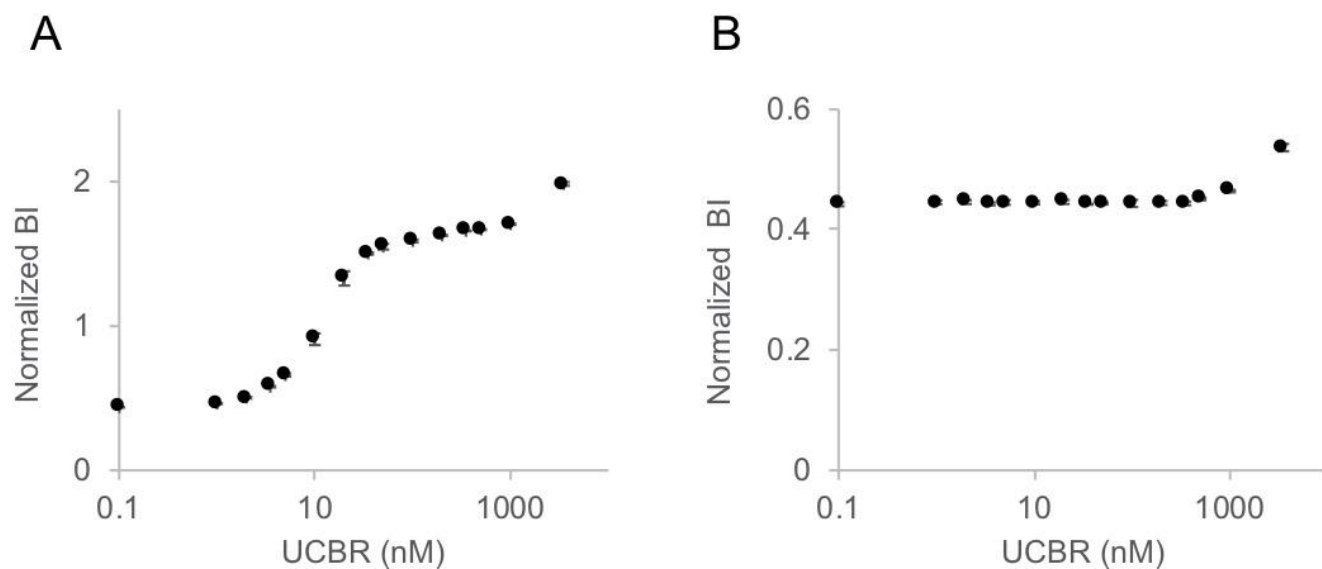
Supplemental Figure 4. Dose-response curve of BABI and Nluc to UCBR. (A) Normalized bioluminescence intensity (Normalized BI) at 530 nm of BABI reacted with several concentrations of UCBR. The intensity was normalized at iso-emissive point (510 nm). (B) Normalized bioluminescence intensity at 530 nm of Nluc reacted with UCBR. The intensity was normalized at 510 nm. The averaged data and standard deviations are shown for $n = 3$
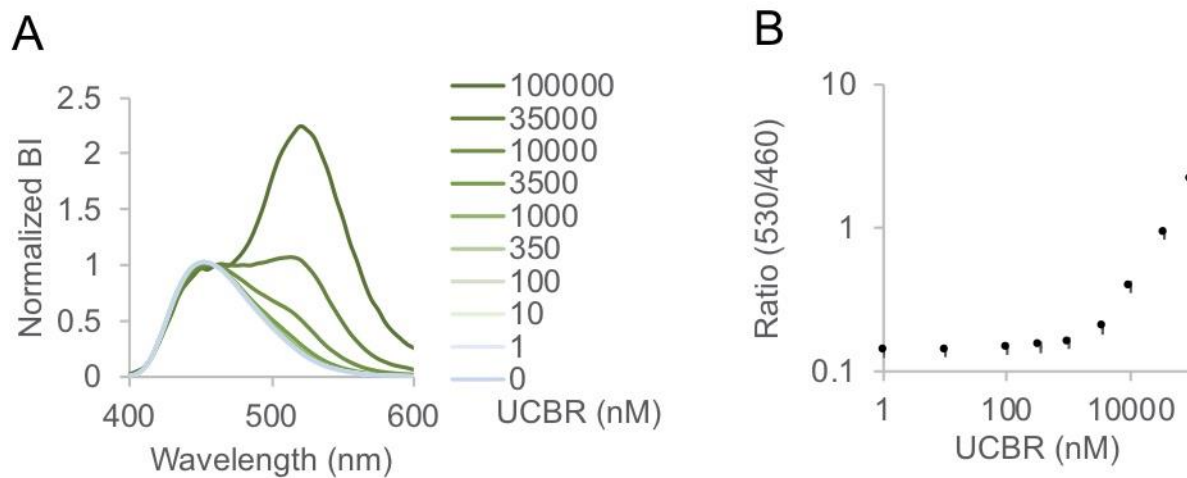
Supplemental Figure 5. Dose-response of Nluc emission to UCBR. (A) The emission spectra of Nluc mixed with several concentrations of UCBR. The intensities were normalized by the intensity at 460 nm. (B) The emission ratio (530/460 nm) calculated from the spectra A. The average and standard deviations are shown for *n* = 3
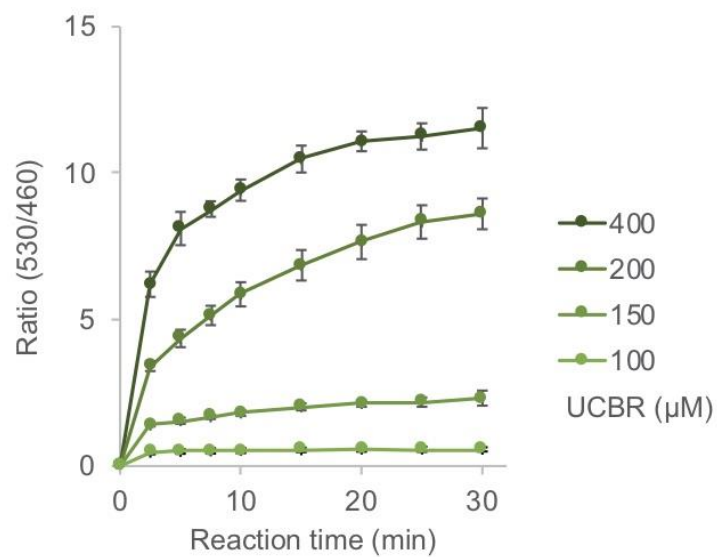
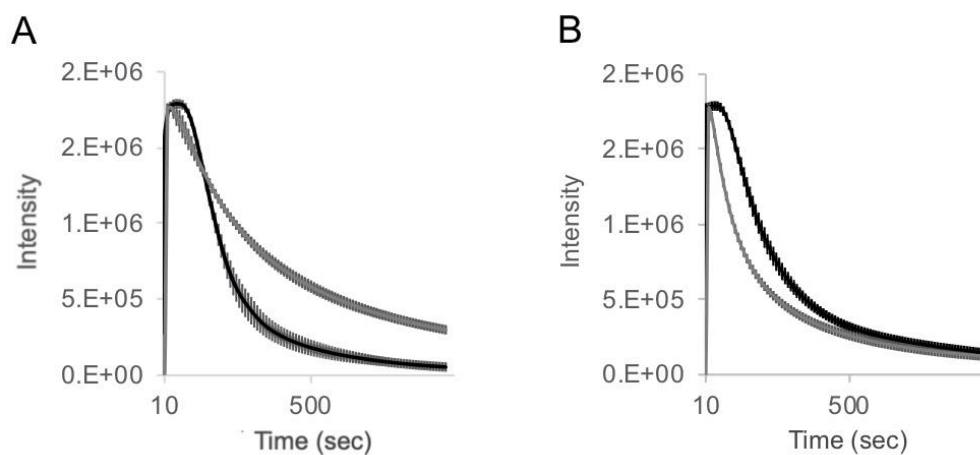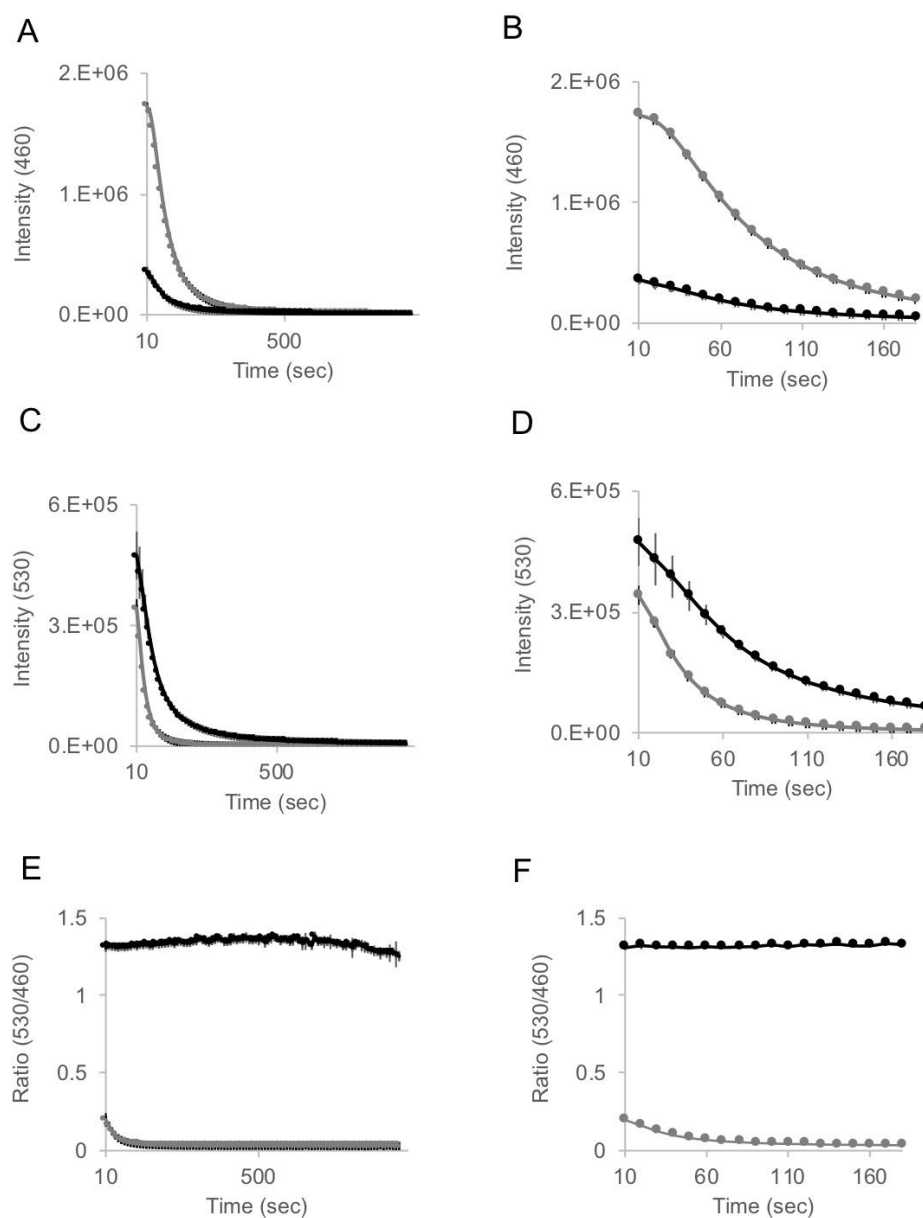**Supplemental Figure 6. Time-dependent changes in the emission ratio of BABI with blood.** The emission ratio (530/460 nm) of BABI reacted with mouse blood spiked with UCBR for several minutes. The average and standard deviations are shown for n = 3.

Supplemental Figure 7. BABI reaction using different substrates. (A) The time-dependent changes in the intensity of BABI with substrates, coelenterazine-h (black) and furimazine (gray) measured by a microplate reader. (B) The time-dependent changes in the intensity of BABI reacted with 3 μL of 200 μM UCBR with substrates, coelenterazine-h (black) and furimazine (gray). The condition of solution is the same with 2 μM BABI in Figure 3A. The average and standard deviations are shown for $n = 3$

Supplemental Figure 8. Time-dependency of the intensity and emission ratio of BABI. The time-dependent intensity of BABI measured using an emission filter for 460 nm (A, B), and for 530 nm (C, D), and the calculated ratio from A and C (E, F). BABI (gray) and BABI reacted with 3 µL of 200 µM UCBR (black) was evaluated. The average and standard deviations are shown for *n* = 3.
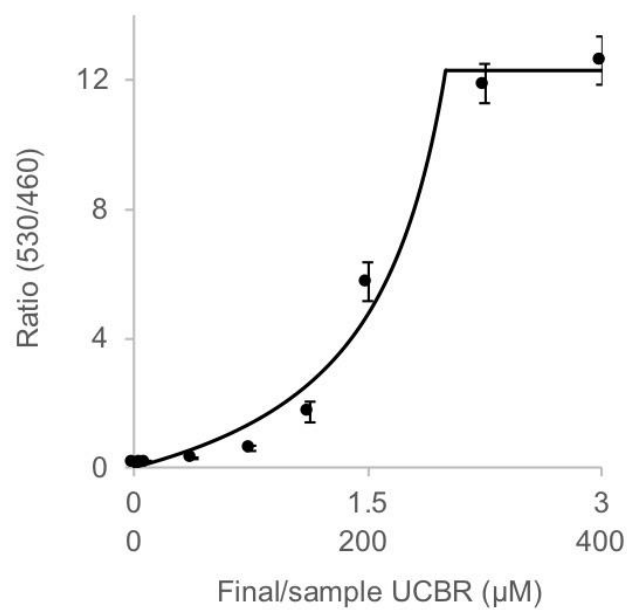
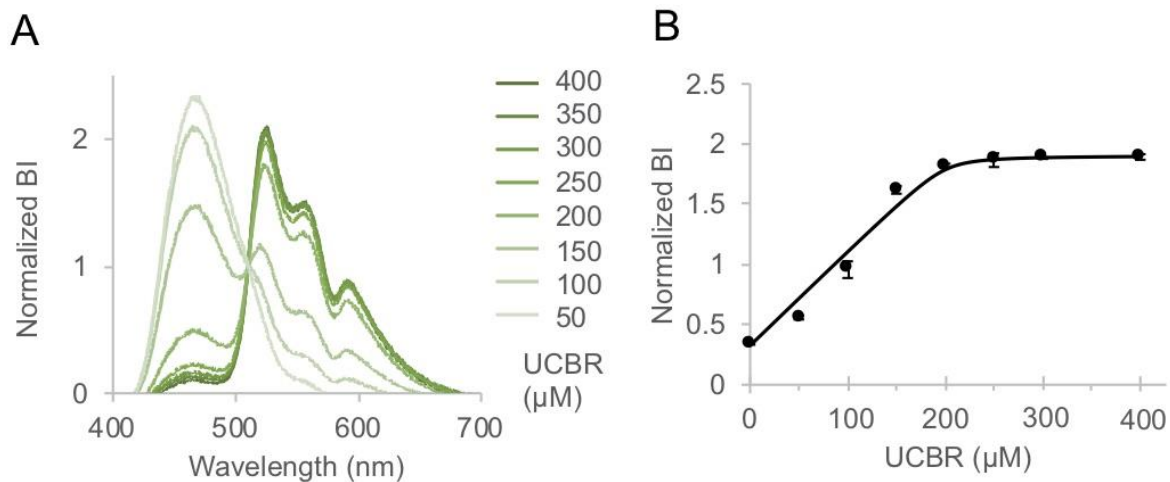**Supplemental Figure 9. Ratio change of BABI by UCBR.** The ratio of bioluminescence intensity (530/460 nm) of 2 μM BABI reacted with several concentrations of UCBR measured by a multichannel spectrophotometer. The fitting curve was calculated according to supplemental Note 2. The averaged data and standard deviations are shown for n = 3
.

Supplemental Figure 10. Emission spectra of BABI reaction with blood spiked with UCBR. (A) Bioluminescent spectra of BABI reaction with mouse blood, measured by a multichannel spectrophotometer. The intensity was normalized at the iso-emissive point. Y-axis shows the normalized bioluminescence intensity (Normalized BI). (B) Changes in the normalized BI of BABI at 530 nm depends on UCBR concentration. The values were calculated from the spectra in A. The averaged data and standard deviations are shown for $n = 3$.
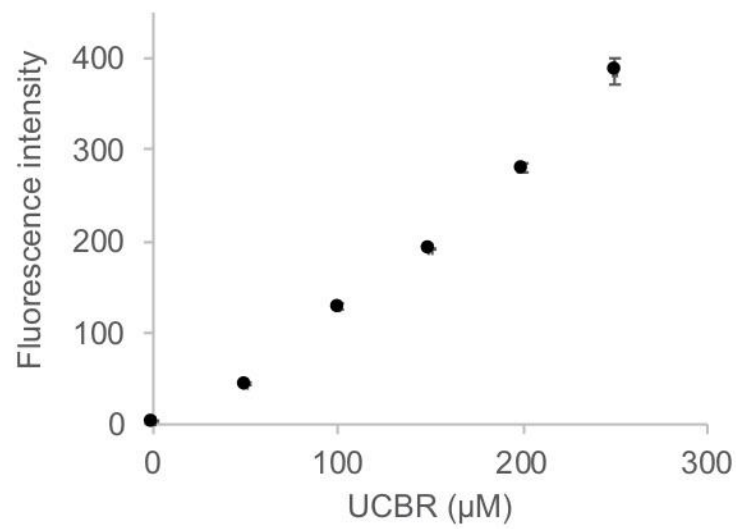
Supplemental Figure 11. UCBR measurement by UnaG. (A) Fluorescence of UnaG reacted with several concentrations of UCBR. The same UCBR spiked mouse blood as in Figure 5 was used. The method of the previous paper (See ref. 18 in main text) was followed in the experiment.

Supplemental Note 1. Analysis for the plots of normalized intensity of BABI.

In this note, we present a mathematical procedure to analyze the binding curve of BABI with UCBR by least squares fitting. In a reaction such that

$$BABI + UCBR \rightarrow BABI \cdot UCBR, \quad [1]$$
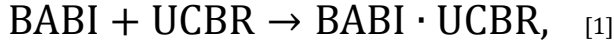
We derive a formulation that calculates the intensity ratio as a function of the total concentration of UCBR added to a sample solution, $[UCBR]_T$. We assume that (1) BABI has a single binding site for UCBR and (2) the dissociation constant K_d of reaction [1] is almost in the same order of or lower than the total concentration of BABI ($K_d \sim [BABI]_T$ or $K_d < [BABI]_T$), where K_d is expressed as

$$K_d = \frac{[BABI][UCBR]}{[BABI \cdot UCBR]}. \quad [2]$$

Assumption (2) suggests that the concentrations of both the unbound form (BABI) and the bound form (BABI·UCBR) are not negligible. Let $[BABI]_T$ be the total concentration of BABI, and we have

$$[BABI]_T = [BABI] + [BABI \cdot UCBR] \quad [3]$$

and

$$[UCBR]_T = [UCBR] + [BABI \cdot UCBR]. \quad [4]$$

Note that [BABI] and [UCBR] are the concentrations of free BABI and UCBR, respectively. From Eqs. [2–4], we can derive the solution of [UCBR] as a function of $[BABI]_T$ and $[UCBR]_T$ given by:

$$[UCBR] = \frac{-(K_d + [BABI]_T - [UCBR]_T) + \sqrt{(K_d + [BABI]_T - [UCBR]_T)^2 + 4K_d[UCBR]_T}}{2}. \quad [5]$$

[UCBR] and K_d are used to express mole fractions of BABI and BABI·UCBR as follows:

$$\alpha_{BABI} = \frac{[BABI]}{[BABI] + [BABI \cdot UCBR]} = \frac{K_d}{K_d + [UCBR]} \quad [6]$$

and

$$\alpha_{BABI \cdot UCBR} = \frac{[BABI \cdot UCBR]}{[BABI] + [BABI \cdot UCBR]} = \frac{[UCBR]}{K_d + [UCBR]}. \quad [7]$$

Let Y_1 and Y_2 be apparent intensities measured at wavelengths λ_1 and λ_2. The mole fractions (Eqs. [6, 7]) are used to express Y_1 and Y_2:

$$Y_1 = A_1 \alpha_{BABI} + B_1 \alpha_{BABI \cdot UCBR} = A_1 \frac{K_d}{K_d + [UCBR]} + B_1 \frac{[UCBR]}{K_d + [UCBR]} \quad [8]$$

and

$$Y_2 = A_2 \alpha_{BABI} + B_2 \alpha_{BABI \cdot UCBR} = A_2 \frac{K_d}{K_d + [UCBR]} + B_2 \frac{[UCBR]}{K_d + [UCBR]}, \quad [9]$$

where A_1 and A_2 are intensities at $\alpha_{BABI} = 1$ at wavelengths of λ_1 and λ_2, respectively, and B_1 and B_2 are intensities at $\alpha_{BABI\text{-}UCBR} = 1$ at wavelengths of λ_1 and λ_2, respectively. Therefore, we have the mathematical expression of the intensity ratio between Y_1 and Y_2 as

$$\frac{Y_1}{Y_2} = \frac{A_1\dfrac{K_d}{K_d+[UCBR]}+B_1\dfrac{[UCBR]}{K_d+[UCBR]}}{A_2\dfrac{K_d}{K_d+[UCBR]}+B_2\dfrac{[UCBR]}{K_d+[UCBR]}} = \frac{A_1 K_d+B_1[UCBR]}{A_2 K_d+B_2[UCBR]}. \qquad [10]$$

In the case in which we take an iso-emissive point for λ_2, Y_2 is constant, that is, $A_2 = B_2$. This simplifies the function of Eq. [10] so that we have the form of

$$\frac{Y_1}{Y_{2(\text{isoemissive})}} = \frac{A_1 K_d+B_1[UCBR]}{A_2 K_d+B_2[UCBR]} = \frac{C K_d+D[UCBR]}{K_d+[UCBR]}. \qquad [11]$$

In the case in which we take a non-iso-emissive point for λ_2, the function of the intensity ratio can also be re-arranged into a single binding isotherm similar to Eq. [11], but the K_d is factored by a coefficient, which needs correction to compute the actual value of K_d.[2] Accordingly, when we have a plot of intensity ratio Y_1/Y_2 as a function of $[UCBR]_T$ measured at a fixed $[BABI]_T$, we perform least squares fitting of the data points with the function in Eq. [10] or [11] in which [UCBR] is given by Eq. [5]. Specifically, in the present case, λ_1 and λ_2 are 530 and 510 nm, respectively.

Supplemental Note 2. A titration curve for the plots of the ratio of intensity at 530 nm to that at 460 nm fitted by Mathematica.

Now we consider the reaction: $BABI + UCBR \rightarrow BABI \cdot UCBR$.
Here, we derive a model function that emulates the ratio of intensity, Y. We assumed that (1) the total concentration of BABI was much higher than the K_d value ($[BABI]_T \gg K_d$) and (2) UCBR concentration is almost in the same order as the total concentration of BABI ($[UCBR]_T \sim [BABI]_T$). These conditions mean that the addition of UCBR leads to the complete formation of BABI-UCBR. Let f be a mole fraction of BABI bound with UCBR to the total BABI. Then, we have

$$f = \frac{[BABI \cdot UCBR]}{[BABI]_T} \approx \min\left(1, \frac{[UCBR]_T}{[BABI]_T}\right). \qquad [12]$$

The most right-hand applies because the amount of UCBR-bound BABI does not exceed the total amount of BABI. Thereby, *the model function Y* is expressed as

$$Y = \frac{(1-f)A_1 + fB_1}{(1-f)A_2 + fB_2}, \qquad [13]$$

where λ_1 and λ_2 are 530 and 460 nm, respectively. Eq. [13] can also be applied to the analysis of the ratio of a signal from the green channel to that of the blue channel, measured by a smartphone camera in the same manner.

Supplemental Note 3. Nucleotide sequence of BABI UnaG is highlighted in green and that of NlucΔ1 is highlighted in cyan.

>BABI: UnaG_NlucΔ1

ATGGTCGAGAAATTTGTTGGCACCTGGAAGATCGCAGACAGCCATAATTTTGGTGAATACCTGAAAGC
TATCGGAGCCCCAAAGGAATTAAGCGATGGTGGGGATGCCACGACGCCGACATTGTACATCTCCCAG
AAGGACGGAGACAAAATGACAGTGAAAATAGAGAATGGACCTCCTACGTTCCTTGACACTCAAGTAAA
GTTCAAATTAGGGGAGGAGTTCGACGAATTTCCTTCTGATCGAAGAAAAGGCGTAAAATCTGTCGTGA
ACTTGGTGGGAGAGAAGCTGGTGTACGTACAAAAGTGGGACGGCAAGGAGACGACGTATGTCCGAG
AGATAAAGGACGGTAAACTGGTCGTGACACTTACGATGGGAGACGTCGTGGCTGTGCGCAGCTACCG
GAGGGCGACGGAAGGTACCGTCTTCACACTCGAAGATTTCGTTGGGGACTGGCGACAGACAGCCGG
CTACAACCTGGACCAAGTCCTTGAACAGGGAGGTGTGTCCAGTTTGTTTCAGAATCTCGGGGTGTCC
GTAACTCCGATCCAAAGGATTGTCCTGAGCGGTGAAAATGGGCTGAAGATCGACATCCATGTCATCAT
CCCGTATGAAGGTCTGAGCGGCGACCAAATGGGCCAGATCGAAAAAATTTTTAAGGTGGTGTACCCT
GTGGATGATCATCACTTTAAGGTGATCCTGCACTATGGCACACTGGTAATCGACGGGGTTACGCCGAA
CATGATCGACTATTTCGGACGGCCGTATGAAGGCATCGCCGTGTTCGACGGCAAAAAGATCACTGTAA
CAGGGACCCTGTGGAACGGCAACAAAATTATCGACGAGCGCCTGATCAACCCCGACGGCTCCCTGCT
GTTCCGAGTAACCATCAACGGAGTGACCGGCTGGCGGCTGTGCGAACGCATTCTGGCGTAA

References

(1) Kunikata, T.; Itoh, S.; Ozaki, T.; Kondo, M.; Isobe, K.; Onishi, S. Formation of propentdyopents and biliverdin, oxidized metabolites of bilirubin, in infants receiving oxygen therapy. *Pediatr Int.* **2000**, 42, 331–336.

(2) Pomorski, A.; Kochańczyk, T.; Miłoch, A.; Krężel, A. Method for Accurate Determination of Dissociation Constants of Optical Ratiometric Systems: Chemical Probes, Genetically Encoded Sensors, and Interacting Molecules Adam. *Anal. Chem.* **2013**, 85, 11479–11486.